Electrochemistry

Deutsche Ausgabe: DOI: 10.1002/ange.201410174
Internationale Ausgabe: DOI: 10.1002/anie.201410174

Sulfur Cathodes Based on Conductive MXene Nanosheets for High-Performance Lithium–Sulfur Batteries**

*Xiao Liang, Arnd Garsuch, and Linda F. Nazar**

Abstract: *Lithium–sulfur batteries are amongst the most promising candidates to satisfy emerging energy-storage demands. Suppression of the polysulfide shuttle while maintaining high sulfur content is the main challenge that faces their practical development. Here, we report that 2D early-transition-metal carbide conductive MXene phases—reported to be impressive supercapacitor materials—also perform as excellent sulfur battery hosts owing to their inherently high underlying metallic conductivity and self-functionalized surfaces. We show that 70 wt % S/Ti_2C composites exhibit stable long-term cycling performance because of strong interaction of the polysulfide species with the surface Ti atoms, demonstrated by X-ray photoelectron spectroscopy studies. The cathodes show excellent cycling performance with specific capacity close to 1200 mA h g^{-1} at a five-hour charge/discharge (C/5) current rate. Capacity retention of 80 % is achieved over 400 cycles at a two-hour charge/discharge (C/2) current rate.*

The rechargeable lithium–sulfur battery has attracted an enormous amount of interest recently owing to its promise of high-energy density at low costs, combined with the high natural abundance of sulfur, and its environmental friendliness.[1] These factors suggest its suitability for meeting the demand of electric vehicles and large-scale renewable energy storage.[2] Next to oxygen, elemental sulfur exhibits the highest theoretical capacity per gram (1675 mA h g^{-1}) among current widely used cathode materials, based on the redox reaction between elemental sulfur and lithium sulfide (Li_2S).[3] However, after almost 30 years of development, the Li-S battery is still not primed for commercialization. The major obstacles are less-than-theoretical use of sulfur, as well as poor cycling life and Coulombic efficiency owing in large part to the dissolution of the intermediate lithium polysulfide (LiPS) species into the organic electrolyte.[4] The dissolved LiPS can chemically react with the lithium anode to form Li_2S on the surface, leading to increased impedance and/or loss of capacity. Although this can be alleviated by adding $LiNO_3$ to the electrolyte to passivate the surface, or using a Li_3N layer to form a protective layer,[5] the active material loss by dissolution still must be addressed. In recent years, sulfur cathodes with optimal porosity and high surface area have been designed to contain polysulfides by physisorbtion. Carbon-based materials, such as mesoporous carbons,[6] graphene[7] and carbon spheres[8] were reported as effective hosts to improve cycling performance.

More recently it has been discovered that surface-functionalized carbon materials such as reduced graphene oxides[9] or polymer-modified mesoporous carbon atoms[6] show much better properties because of their hydrophilic surfaces which bind LiPSs by chemisorption. Metal oxides, including SiO_2,[10] TiO_2,[11] and Al_2O_3,[12] which are inherently hydrophilic because of the polar metal–O bond, have also been reported to be effective LiPS absorbents. High surface area, polar metallic porous oxides such as Ti_4O_7 have been used as a two-in-one approach to provide both a "sulfiphilic" surface and electron transport to effect surface-enhanced redox chemistry and extend cycle life,[13] or to spatially locate Li_2S deposition on conductive indium tin oxide by strong hydrophilic surface interactions.[14] Chemical adsorption or bonding of polysulfides to host materials through P–S bonds,[15] O–S bonds,[16] and Ti–S bonds[17] provides a multitude of new strategies to suppress the polysulfide shuttle.

Here we report on a new class of sulfur host materials—the so-called delaminated MXene phases—that capitalize on a combination of inherently high conductivity and highly active 2D surfaces to chemically bond intermediate polysulfides by metal–sulfur interactions. MXenes are an exciting family of early-transition-metal carbides or carbonitrides first reported by Gogotsi et al. in 2011.[18] They are produced by selective etching of the A element in aqueous HF from the MAX phases,[19] named because of their composition $M_{n+1}AX_n$; where M is an early transition metal, A is a group IIIA or IVA element, X is C and/or N, and $n = 1$, 2, or 3.[20] These phases form highly exfoliated sheets. The average thickness for Ti_3AlC_2 corresponds to about 10 layers and some OH^- may be replaced by F^-.[19] Delamination of the sheets is effected via solvation by donor solvents.[21] The resultant nanosheets, described as $Ti_3C_2(OH)_xO_yF_z$ for the Ti_3C_2 parent phase, can be considered as "inorganic graphene oxides". These materials have been used as supercapacitors,[22] where their high volumetric capacitance has caught the attention of researchers worldwide. Although both supercapacitors and batteries are vital for energy storage,[23] their electrochemical characteristics are quite different.[24] Little has been reported for MXene phases for batteries, except as Li(Na)-ion anode materials.[25,26]

[*] Dr. X. Liang, Prof. Dr. L. F. Nazar
Department of Chemistry, University of Waterloo
200 University Avenue West, Waterloo
Ontario, N2L 3G1 (Canada)
E-mail: lfnazar@uwaterloo.ca
Dr. A. Garsuch
BASF SE, Ludwigshafen, 67056 (Germany)

[**] This research was supported by the BASF International Scientific Network for Electrochemistry and Batteries. We thank NSERC for generous support via a Canada Research Chair to L.F.N., and Dr. Marine Cuisinier for helpful discussions. MXene = early-transition-metal carbide.

Supporting information for this article is available on the WWW under http://dx.doi.org/10.1002/anie.201410174.

We demonstrate here for the first time that the MXene phase Ti_2C is highly effective as a cathode host material for sulfur batteries, providing very stable cycling performance and high capacity even with 70 wt% S. This material, and the 60 other members of the MXene family, couple the advantage of high 2D electron conductivity of transition-metal carbides (much higher than graphene oxide) and exposed terminal metal sites that bind the sulfides (Scheme 1). As revealed by X-ray photoelectron spectroscopy (XPS) analysis, sulfur/sulfide species replace the hydroxy groups, forming a strong Ti-S interaction with the core (Scheme 1).

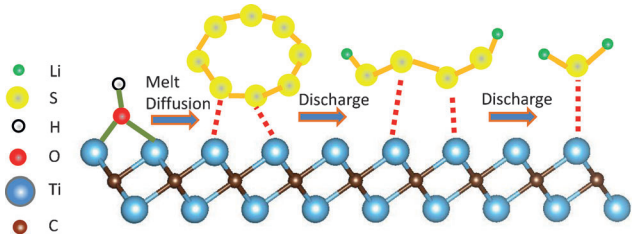

Scheme 1. Replacement of the Ti-OH bond on the MXene surface with a S-Ti-C bond on heat treatment or by contact with polysulfides.

To prepare the host, we chose a common MAX phase (Ti_2AlC, Figure S1 in the Supporting Information) and etched away the Al atoms by hydrofluoric acid treatment to give exfoliated e-Ti_2C (Figure 1a).[27] Delamination in DMSO formed Ti_2C 2D nanosheets (d-Ti_2C, Figure 1b) as reported.[21] This was confirmed by N_2 surface area measurements that showed an increase from 20.2 $m^2 g^{-1}$ for stacked e-Ti_2C to 67.9 $m^2 g^{-1}$ of d-Ti_2C (Figure S2). Details of the synthesis and characterization are provided in the Supporting Information.

Sulfur was incorporated into the Ti_2C matrix by melt diffusion, using nanosized sulfur particles to obtain a homogenous mixture before heat treatment (see Experimental Section). Effective delamination is critical. Significant sulfur aggregation was observed after melt diffusion in non-delaminated e-Ti_2C (Figure 1c), which results in loss of sulfur by evaporation on heat treatment, to give only 63 wt% sulfur in the composite (Figure S3). Conversely, sulfur incorporation on the surface of the delaminated Ti_2C sheets (d-Ti_2C) was achieved with no apparent inhomogeneity (Figure 1d); indicating excellent sulfur dispersion. Accordingly, thermogravimetric analysis (TGA) showed that all of the sulfur is retained in the S/d-Ti_2C sample after melt-diffusion, yielding a 70 wt% composite (Figure S3).

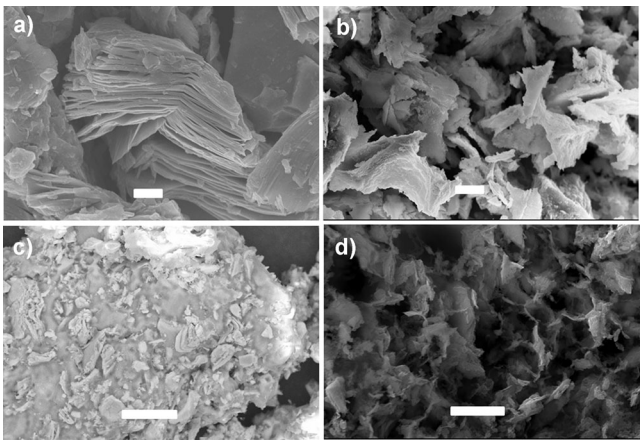

Figure 1. SEM images of a) e-Ti_2C, b) d-Ti_2C, c) S-impregnated e-Ti_2C showing Ti_2C particles immersed in solid sulfur, and d) sulfur-impregnated d-Ti_2C. Scale bar = 1 μm in (a) and (b); and 10 μm in (c) and (d).

Electrochemical performance of the 70S/Ti_2C composite cathodes was examined in coin cells. Typical sulfur redox was observed for both of the S/Ti_2C composites, with two reduction plateaus in the first activation discharge at C/20 (Figure 2 and Figure S4a). The predictably poor electrochemical performance of the highly sulfur-aggregated 63S/e-Ti_2C is displayed in Figure S4a: after a high discharge capacity of 1350 mA h g^{-1}, a significant capacity (ca. 190 mA h g^{-1}) was not recovered during the following charge, suggesting extensive loss of active material into the electrolyte. Accordingly, its long term cycling performance at C/2 faded from 965 mA h g^{-1} to 460 mA h g^{-1} at the 100th cycle (Figure S4b). This owes to the very poor surface contact of the sulfur/sulfides with the $Ti_2C(OH)_x$ surface. Conversely, 70S/d-Ti_2C from delaminated Ti_2C showed excellent cycling stability at various rates, as shown in Figure 2 and Figure S5a. 70S/d-Ti_2C delivered a discharge capacity of 1090 mA h g^{-1} at a C/2 rate (837 mA g^{-1}) while at 1C (1675 mA g^{-1}) the discharge capacity was still 1000 mA h g^{-1}. Following an activation cycle, all cells showed excellent capacity retention up to the

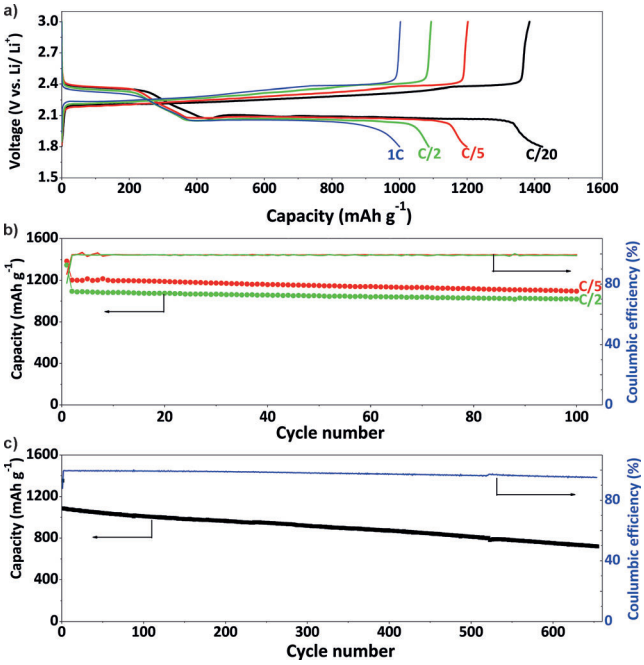

Figure 2. a) Voltage profiles of 70S/d-Ti_2C at various rates ranging from C/20 to 1C. b) Cycling performance of 70S/d-Ti_2C at C/5 and C/2. c) Long-term cycling at C/2. Cells were conditioned for the first cycle at C/20 to facilitate electrode wetting. The increase in rate on the 2nd cycle results in the change in capacity.

100th cycle. Long term cycling of 70S/d-Ti_2C at C/2 is demonstrated in Figure 2c. The 70S/d-Ti_2C achieves very stable performance with a discharge capacity of 723 mA h g^{-1} after 650 cycles, corresponding to a decay rate of 0.05% per cycle. While this is not the very lowest decay rate reported—values ranging between 0.028% and 0.07% have been recorded recently for sulfur hosts based on N,S-doped graphene oxide;[28] graphene oxide in combination with specialty binders and viscous electrolytes;[9] egg yolk-shell TiO_2;[29] and Ti_4O_7[13,14]—this places the MXene squarely in the middle of the highest performing materials: even without optimization. Comparison of fade rates is made difficult in the light of different current rates, sulfur loading and cycle ranges that are employed in different reports.

The 70S/d-Ti_2C composite was cycled at various current rates to probe its response, as shown in Figure S5b. The cell stabilized at 1040 mA h g^{-1} at C/5 over 20 cycles before being subjected to current densities ranging from C/2 to 4C. A capacity of 660 mA h g^{-1} was achieved at the highest 4C rate. Upon step-wise decrease of the current density to C/5, 960 mA h g^{-1} capacity was recovered after 100 cycles, corresponding to 92% of the initial capacity and indicative of the robustness of the cathode.

Compared to many other sulfur host materials used to trap polysulfides,[6–9,14–16] two dimensional MXene Ti_2C nanosheets have neither particularly high surface area (67.9 $m^2 g^{-1}$) nor a well-ordered pore structure. Nonetheless, they clearly exhibit excellent properties as a sulfur host, implying they function effectively to depress the polysulfide shuttle. Although all of the sulfur/sulfide in the cell cannot cover the interface as a monolayer, this is not required for an interaction that derives from chemisorption (versus physisorption), as we show below. The Ti_2C nanosheets are unique in possessing functional oxygen surface groups owing to exfoliation and delamination (which replaces the Al in Ti_2AlC with OH groups);[18] surface Ti atoms with unoccupied orbitals; and an underlying delocalized band structure that gives rise to metallic conductivity. X-ray photoelectron spectroscopy (XPS) analysis was used to identify the surface chemical environment of the sulfur–Ti_2C composite, both in the pristine material and upon cycling. This probe of the surface interaction reveals its chemisorptive nature.

In d-Ti_2C itself, the Ti 2p XPS spectrum shows two predominant Ti $2p_{3/2}$ peaks at 455.9 and 459.4 eV (Figure 3 a_i) which are attributed to Ti-C in the core and Ti-O on the surface, respectively.[21] The latter is ascribed to the native oxide (Ti-O-Ti) of the starting MAX phase (Ti_2AlC) formed by exposure of the material to air.[30] However, the surface of Ti_3C_2 is covered with an abundance of hydroxy groups (Ti-OH), to form "$Ti_2C_3(OH)_2$".[18] By extension, these are also proposed to describe the Ti_2C surface.[27] In accord, we observe two O environments of the Ti_2C by O1s XPS (Figure S6a): an O 1s peak ascribed to Ti-O-Ti at 530.4 eV[21] and one ascribed to Ti-OH at 532.1 eV.[31] Note that only the binding energy of the $2p_{3/2}$ component of the $2p_{3/2}/2p_{1/2}$ spin doublet is stated, following convention.

The 70S/d-Ti_2C composite exhibits the same predominant Ti 2p environment, along with a new Ti $2p_{3/2}$ peak at 457.6 eV that is assigned to a S-Ti-C bond (Figure 3 a_{ii}). The Ti binding

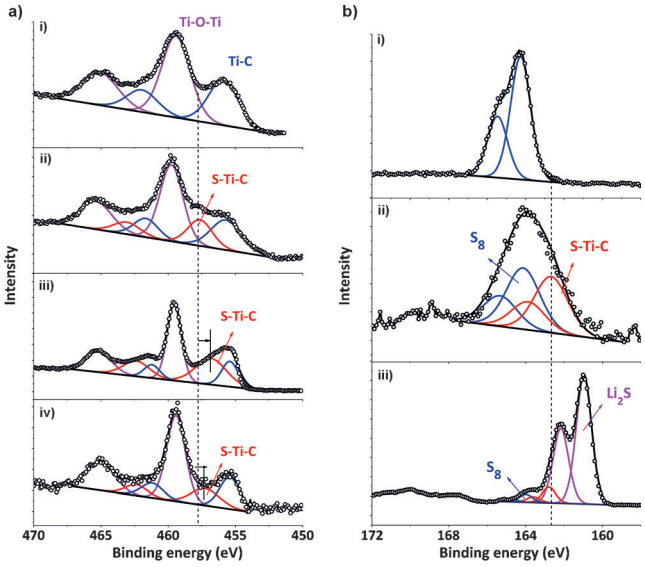

Figure 3. XPS analysis of the Ti_2C sheets and S/Ti_2C composite. a) Ti 2p spectra of the i) Ti_2C sheets and ii) 70S/Ti_2C composite, iii) Li_2S_4-Ti_2C and iv) 70S/Ti_2C electrode discharged to 1.8 V at C/20, in DOL/DME (1:1 vol%) electrolyte with 1 M $LiClO_4$. b) S 2p spectra of i) elemental sulfur, ii) 70S/Ti2C composite, and iii) 70S/Ti_2C electrode discharged to 1.8 V at C/20. Binding energies were calibrated to the C 1s peak at 285 eV.

energy is only 0.7 eV higher than that of TiS_2.[32] The small shift can be attributed to the electronic effect of the underlying metallic carbide and asymmetric environment of the surface Ti atoms. Accordingly, in addition to the elemental sulfur (S_8) detected in the S 2p spectrum of the 70S/Ti_2C, an additional S $2p_{3/2}$ peak of the same intensity appears at 162.5 eV (Figure 3 b_{ii}), which lies exactly in the range of the published Ti-S binding energy of Ti–S bonds (ca. 162.3 ± 0.2 eV).[33] This indicates that the MXene Ti_2C nanosheet Ti-OH groups are replaced by sulfur (or S^{2-}) at elevated temperature during the heat treatment to infuse the sulfur.

This is confirmed by the decreased Ti-OH fraction in the 70S/Ti_2C composite (26% compared to 57% in pristine Ti_2C, as determined by O 1s XPS, see Figure S6b). The electronegative S atoms lead to a decrease in electron density of the Ti atom, resulting in a higher binding energy compared to the Ti–C bond. This can be explained in terms of a Lewis acid–base interaction which involves unoccupied orbitals of the surface Ti atoms. These atoms coordinate with an electron donating host (sulfur species in this case). This concept has been previously used to account for the strong interactions between the Ni^{2+} ions in insulating metal–organic frameworks and lithium polysulfides.[34] A significant advantage here is that the underlying host exhibits very high conductivity. The MAX phases are metallic, and a "clean" single MXene sheet is also predicted to be metallic. MXene phases with hydroxy functionalization have very low resistivity (0.03 μΩ m), behaving as semiconductors with a very small band gap of 0.05 eV.[18]

To illustrate the interaction between lithium polysulfides and Ti_2C, with an aim to simulate the environment in a Li/S cell, d-Ti_2C nanosheets were contacted with a representative

lithium polysulfide solution (Li_2S_4; see the Experimental Section). The Ti 2p XPS spectrum of the mixture again shows the additional feature indicative of a Ti–S bond, but now with a binding energy 0.8 eV lower than that of the S-Ti-C interaction described for 70S/Ti_2C (Figure 3 a_{iii}). This is explained by the fact that the nucleophilic polysulfides donate electron density to the Ti, thus slightly lowering the binding energy. The presence of the S-Ti-C bond at 467.2 eV is also evidenced in the Ti 2p XPS spectrum of the fully discharged S/Ti_2C electrode (Figure 3 a_{iv}). The S 2p spectrum shows that the predominant sulfur environment is Li_2S (Figure 3 b_{iii}), together with 4% S_8 (164.2 eV) and 10% S-Ti-C (162.5 eV). The capacity based on 86% Li_2S is calculated to be 1440 mA h g^{-1}, very similar to the actual capacity (1422 mA h g^{-1}), implying polysulfides were efficiently trapped during the discharge process.

The above analysis confirms that the sulfide discharge products form a good interface with the Ti_2C nanosheets. As shown in Figure S7, Li_2S particles appear to be homogeneously deposited on the Ti_2C surface. To further illustrate the significant role of interfacial interaction on the suppression of the polysulfide shuttle, cells without $LiNO_3$ additive in the electrolyte were also examined. Greatly improved average Coulombic efficiency (ca. 94% for 70S/Ti_2C versus 70% for 70S/KB (Ketjenblack) composite) was demonstrated (Figure S8).

In summary, we have shown that highly conductive carbide Ti_2C 2D nanosheets with a hydrophilic surface are effective as a sulfur host for Li-S batteries. A highly uniform positive electrode comprised of 70S/d-Ti_2C was created by reacting sulfur with the hydroxlated surface of the Ti_2C nanosheets. The existence of S-Ti-C bonding at the interface determined by XPS analysis is suggestive of strong interaction and chemisorption of polysulfides onto the "acid" Ti sites and hydroxy surface groups. These sites act as active species. In a cell, we propose the initially sorbed polysulfides would undergo conversion to Li_2S—either by electron transfer via the Ti_2C or by disproportionation—to form multiple Li_2S nucleation sites on the surface. As progressive consumption of sulfur generates more polysulfides, these are reduced to sulfide which would preferentially deposit epitaxially on the existing Li_2S nuclei. This effectively mitigates the dissolution of polysulfides into the electrolyte and provides very good cycling performance with a capacity fade rate of 0.05% per cycle. Thus, we believe that interface-mediated reduction of the LiPS plays a major role in inhibiting the loss of active materials as previously reported,[13] and may even be more effective for hydroxylated Ti-carbide surfaces than for oxides. These results indicate that other MXene phases (over 60 are known) will also be highly promising candidates for high-performance Li-S batteries. Indeed, in our laboratory, we have found that other MXenes such as Ti_3C_2, Ti_3CN and V_2C display similar properties, as we will report subsequently.[35]

Experimental Section

Preparation of S/Ti_2C composite: To load sulfur into the Ti_2C, nano-sized sulfur was synthesized by reacting 255 mg $Na_2S_2O_3$ with 278 μL concentrated HCl and 17 mg polyvinylpyrrolidone (Sigma–Aldrich) in 85 mL DI water. Uniform nanoparticles ≈400 nm in dimension were obtained (Figure S9). Suspensions of Ti_2C (e-Ti_2C or d-Ti_2C) and nano-sized sulfur were mixed to provide a weight ratio of Ti_2C:S of 3:7. S/Ti_2C composites were obtained by heating the mixtures at 155 °C overnight.

Preparation of Ti_2C-Li_2S_4: Delaminated Ti_2C was dried at 90 °C under vacuum for overnight) prior to use, and 0.5 mmol of the Ti_2C was combined with 5 mL of 0.1 M Li_2S_4 (see SI) in DME. The mixture was stirred for 2 h, centrifuged and dried under vacuum overnight.

Electrochemical measurements: Cathodes were prepared from a 80:10:10 mixture of 70S/Ti_2C: Super P: PVDF. Electrochemical studies employed electrodes with an average *active sulfur* loading about 1.0 mg cm^{-2}. Cells were operated in a voltage window of 1.8–3.0 V (except for high rate studies) with 50 μL of electrolyte comprised of 1 M LiTFSI in 1:1 1,2-dimethoxyethane/1,3-dioxolane (DME/DOL; vol%), and 2 wt% $LiNO_3$. Specific capacity values were calculated with respect to the mass of sulfur. Electrodes for XPS analysis were prepared by discharging the coin cell at C/20 to 1.8 V in 1 M $LiClO_4$ (to avoid sulfur contributions from LiFTSI) in a 1:1 v/v ratio of DOL and DME.

See the Supporting Information for details.

Keywords: electrochemistry · energy storage · lithium–sulfur batteries · metallic nanosheets · metal oxides

Zitierweise: *Angew. Chem. Int. Ed.* **2015**, *54*, 3907–3911
Angew. Chem. **2015**, *127*, 3979–3983

[1] Y. Yang, G. Y. Zheng, Y. Cui, *Chem. Soc. Rev.* **2013**, *42*, 3018–3032.
[2] M. Armand, J. M. Tarascon, *Nature* **2008**, *451*, 652–657.
[3] D. Peramunage, S. Licht, *Science* **1993**, *261*, 1029–1032.
[4] Y. V. Mikhaylik, J. R. Akridge, *J. Electrochem. Soc.* **2004**, *151*, A1969–A1976.
[5] G. Q. Ma, Z. Y. Wen, M. F. Wu, C. Shen, Q. S. Wang, J. Jin, X. W. Wu, *Chem. Commun.* **2014**, *50*, 14209–14212.
[6] X. L. Ji, K. T. Lee, L. F. Nazar, *Nat. Mater.* **2009**, *8*, 500–506.
[7] L. Ji, M. Rao, H. Zheng, L. Zhang, Y. Li, W. Duan, J. Guo, E. J. Cairns, Y. Zhang, *J. Am. Chem. Soc.* **2011**, *133*, 18522–18525.
[8] G. He, S. Evers, X. Liang, M. Cuisinier, A. Garsuch, L. F. Nazar, *ACS Nano* **2013**, *7*, 10920–10930.
[9] M. K. Song, Y. G. Zhang, E. J. Cairns, *Nano Lett.* **2013**, *13*, 5891–5899.
[10] X. L. Ji, S. Evers, R. Black, L. F. Nazar, *Nat. Commun.* **2011**, *2*, 325–331.
[11] S. Evers, T. Yim, L. F. Nazar, *J. Phys. Chem. C* **2012**, *116*, 19653–19658.
[12] J. R. Smith, F. C. Walsh, R. L. Clarke, *J. Appl. Electrochem.* **1998**, *28*, 1021–1033.
[13] Q. Pang, D. Kundu, M. Cuisinier, L. F. Nazar, *Nat. Commun* **2014**, DOI: 10.1038/ncomms5759.
[14] H. B. Yao, G. Y. Zheng, P. C. Hsu, D. S. Kong, J. J. Cha, W. Y. Li, Z. W. Seh, M. T. McDowell, K. Yan, Z. Liang, V. K. Narasimhan, Y. Cui, *Nat. Commun.* **2014**, DOI: 10.1038/ncomms4943.
[15] Z. Lin, Z. C. Liu, W. J. Fu, N. J. Dudney, C. D. Liang, *Angew. Chem. Int. Ed.* **2013**, *52*, 7460–7463; *Angew. Chem.* **2013**, *125*, 7608–7611.
[16] J. X. Song, T. Xu, M. L. Gordin, P. Y. Zhu, D. P. Lv, Y. B. Jiang, Y. S. Chen, Y. H. Duan, D. H. Wang, *Adv. Funct. Mater.* **2014**, *24*, 1243–1250.
[17] Z. Liang, G. Zheng, W. Li, Z. W. She, H. Yao, K. Yan, D. Kong, Y. Cui, *ACS Nano* **2014**, *8*, 5249–5256.
[18] M. Naguib, M. Kurtoglu, V. Presser, J. Lu, J. J. Niu, M. Heon, L. Hultman, Y. Gogotsi, M. W. Barsoum, *Adv. Mater.* **2011**, *23*, 4248–4253.
[19] M. Naguib, V. N. Mochalin, M. W. Barsoum, Y. Gogotsi, *Adv. Mater.* **2014**, *26*, 992–1005.

[20] M. W. Barsoum, *MAX Phases: Properties of Machinable Ternary Carbides and Nitrides*, Wiley, Weinheim, **2013**.
[21] O. Mashtalir, M. Naguib, V. N. Mochalin, Y. D. Agnese, M. Heon, M. W. Barsoum, Y. Gogotsi, *Nat. Commun.* **2013**, *4*, 1716.
[22] M. R. Lukatskaya, O. Mashtalir, C. E. Ren, Y. Dall'Agnese, P. Rozier, P. L. Taberna, M. Naguib, P. Simon, M. W. Barsoum, Y. Gogotsi, *Science* **2013**, *341*, 1502 – 1506.
[23] H. D. Yoo, E. Markevich, G. Salitra, D. Sharon, D. Aurbach, *Mater. Today* **2014**, *3*, 110 – 121.
[24] P. Simon, Y. Gogotsi, B. Dunn, *Science* **2014**, *343*, 1210 – 1211.
[25] M. Naguib, J. Come, B. Dyatkin, V. Presser, P. L. Taberna, P. Simon, M. W. Barsoum, Y. Gogotsi, *Electrochem. Commun.* **2012**, *16*, 61 – 64.
[26] D. Er, J. Li, M. Naguib, Y. Gogotsi, V. Shenoy, *ACS Appl. Mater. Interfaces* **2014**, *6*, 11173 – 11179.
[27] M. Naguib, O. Mashtalir, J. Carle, V. Presser, J. Lu, L. Hultman, Y. Gogotsi, M. W. Barsoum, *ACS Nano* **2013**, *6*, 1322 – 1331.
[28] Y. C. Qiu, W. F. Li, W. Zhao, G. Z. Li, Y. Hou, M. N. Liu, L. S. Zhou, F. M. Ye, H. F. Li, Z. H. Wei, S. H. Yang, W. H. Duan, Y. F. Ye, Z. H. Guo, Y. G. Zhang, *Nano Lett.* **2014**, *14*, 4821 – 4827.
[29] Z. W. Seh, W. Li, J. J. Cha, G. Zheng, Y. Yang, M. T. McDowell, P. C. Hsu, Y. Cui, *Nat. Commun.* **2013**, *4*, 1331 – 1336.
[30] S. Myhraa, J. A. A. Crossley, M. W. Barsoum, *J. Phys. Chem. Solids* **2001**, *62*, 811 – 817.
[31] J. C. Yu, J. G. Yu, H. Y. Tang, L. Z. Zhang, *J. Mater. Chem.* **2002**, *12*, 81 – 85.
[32] X. B. Chen, P. A. Glans, X. F. Qiu, S. Dayal, W. D. Jennings, K. E. Smith, C. Burda, J. H. Guo, *J. Electron Spectrosc. Relat. Phenom.* **2008**, *162*, 67 – 73.
[33] H. F. Franzen, M. X. Umaña, J. R. McCreary, R. J. Thorn, *J. Solid State Chem.* **1976**, *18*, 363 – 368.
[34] J. M. Zheng, J. Tian, D. X. Wu, M. Gu, W. Xu, C. M. Wang, F. Gao, M. H. Engelhard, J. G. Zhang, J. Liu, J. Xiao, *Nano Lett.* **2014**, *14*, 2345 – 2352.
[35] X. Liang, A. Garsuch, L. F. Nazar, manuscript in preparation.

Received: October 16, 2014
Published online: February 3, 2015

